Hindawi
Mathematical Problems in Engineering
Volume 2022, Article ID 8499597, 9 pages
https://doi.org/10.1155/2022/8499597

Research Article

Digital Evaluation of Vertical Compressive Bearing Capacity for Jet Grouting Pile-Mini Steel Pipe Pile Composite Foundation

Xiaojun Wang,[1] **Zhipeng Mao**,[2] **and Wendi Wang**[3]

[1]*School of Civil Engineering and Architecture, NingboTech University, Ningbo, Zhejiang, China*
[2]*Zhejiang Wenzhou Yongtaiwen Expressway Co Ltd, Wenzhou, Zhejiang, China*
[3]*Ningbo Architectural Design and Research Institute Co Ltd, Ningbo, Zhejiang, China*

Correspondence should be addressed to Xiaojun Wang; wangxj@nit.zju.edu.cn

Received 15 March 2022; Revised 15 April 2022; Accepted 19 April 2022; Published 11 May 2022

Academic Editor: Zhihan Lv

The jet grouting pile-mini steel pipe pile in soft soil area is composed of the jet grouting pile and the mini steel pipe pile. Through the analysis of the stress mode of the composite foundation under the overall compression of the pile top, the hypothetical diagram and calculation equation of the interfacial friction resistance distribution of the composite foundation are put forward. Thus, the calculation equation of the axial force of the mini steel pipe pile and the jet grouting pile is deduced, and the axial force distribution diagram of the mini steel pipe pile and the jet grouting pile in the composite foundation is defined. The vertical compression composite foundation in the field was selected for bearing capacity test and calculation and comparative analysis, and the relative error was 3%. Therefore, the stress mode and calculation method of the jet grouting pile-mini steel pipe pile proposed in this paper can meet the needs of engineering design and popularization and application of the composite foundation.

1. Introduction

The jet grouting pile-mini steel pipe pile composite foundation refers to the combined system formed by the jet grouting pile and the mini steel pipe pile to share external load [1]. In the soft soil layer, the jet grouting pile with a certain depth and diameter shall be constructed first. Before the initial solidification of the jet grouting pile [2], the mini steel pipe pile with diameter less than Φ300 mm and length less than the length of the jet grouting pile is vertically pushed into the jet grouting pile along the central part by the improved microinserting and pressing mechanical equipment. After the strength of the jet grouting pile reaches 28 days, the composite foundation is formed [3]. In this combined system, the pile top load is mainly transmitted to the jet grouting pile through the friction around the mini steel pipe pile [4], and then the load is transmitted to the soil around the pile mainly by the friction force around the jet grouting pile [5] so as to complete the load transmission [6]. This system can take maximum advantage of the "high strength" characteristics of mini steel pipe pile to bear the load [7] and use the reinforcement effect of jet grouting pile on soft soil and large pile side surface area to provide sufficient side friction resistance [8]. Although the load plate test is more appropriate to discuss the bearing capacity of the composite foundation [9], its deformation and load transfer law cannot be directly extended to the actual engineering design. Therefore [10], it is necessary to study and give a reasonable and simple calculation method of the bearing capacity of the composite foundation [11] so as to make the composite foundation better popularized in engineering application [12], which is the main scientific and technological problem to be solved in this paper. The composite foundation is used in the foundation reinforcement project with the engineering geological condition of soft soils. For the convenience of description, the jet grouting pile-mini steel pipe pile composite foundation is abbreviated as the composite foundation.

2. Stress Mode Analysis of the Composite Foundation under Vertical Compressive Load

It is assumed that in the composite foundation, the uniformity of the jet grouting pile is good [13], and the diameter of the pile body remains unchanged in the depth direction. The mini steel pipe pile and the composite foundation are regarded as pure friction piles, and the bottom axial force is considered as 0. Figure 1 is a schematic diagram of the force transfer mechanism of the composite foundation under vertical compressive load. According to the vertical force transfer characteristics of the composite foundation shown in Figure 1, the composite foundation can be divided into upper and lower parts of "inserted mini steel pipe pile section" and "pure jet grouting pile section" along the depth direction. Due to the small rigidity of the jet grouting pile, when the length of the pure jet grouting pile section is large, the side friction resistance of the "pure jet grouting pile section" mainly acts on the "effective section of the pure jet grouting pile" with the length of L_c. The side friction resistance between the non-effective section at the bottom of the jet grouting pile and soil around the pile is very small, which can be ignored. Therefore, in the calculation of bearing capacity, the effective length of the "pure jet grouting pile section" in the composite foundation should be guaranteed as far as possible so as to reduce the length of the mini steel pipe pile. It is generally believed that the effective pile length of the jet grouting pile shall not exceed 10 m. Combined with the concept of effective pile length of jet grouting pile, the value of the "effective section of pure jet grouting pile" L_c in the composite foundation can be obtained by the following equation:

$$L_c = L_j - L_s \le \min\left\{\beta D_j, 10\right\}. \tag{1}$$

In the formula, L_c is the length of the "effective section of the pure jet grouting pile"; L_j is the effective length of the jet grouting pile; L_s is the length of the mini steel pipe pile. According to the strength of the jet grouting pile body, $\beta = 10 \sim 18$. D_j is the diameter of the jet grouting pile.

Under the overall compression mode of the mini steel pipe pile and jet grouting pile jointly bearing the upper load, the bearing performance of the mini steel pipe pile and the jet grouting pile should be considered at the same time [14, 15].

The ultimate compressive bearing capacity of the mini steel pipe pile at the pile top shall meet the following equation:

$$Q_{0s} \le Q_{su} = \sigma_{su} A_s. \tag{2}$$

The load shared by the top of the jet grouting pile can be calculated according to the following formula:

$$Q_{ju} \ge Q_{0j} = \frac{Q_{su} A_j}{A_s n_p}, \tag{3}$$

$$A_j = \begin{cases} \left(D_j^2 - D_s^2\right)\dfrac{\pi}{4} & (0 < Z < L_s), \\ D_j^2 \dfrac{\pi}{4} & (L_s \le Z). \end{cases} \tag{4}$$

In the equation, Q_{0s} is the compressive load shared by the pile top of the mini steel pipe pile; Q_{0j} is the compressive load shared by the top of the jet grouting pile; Q_{su} is the vertical ultimate compressive bearing capacity of the mini steel pipe pile controlled by yield strength; Q_{ju} is the vertical ultimate compressive bearing capacity of the jet grouting pile without confined compressive strength control; σ_{su} is the yield strength of the mini steel pipe pile; A_s is the cross-sectional area of the mini steel pipe pile, $A_s = \pi(T_s D_s - T_s^2)$, where T_s is the wall thickness of the mini steel pipe pile, and D_s is the outer diameter of the mini steel pipe pile; D_j is the diameter of the jet grouting pile; $n_p = \sigma_{0s}/\sigma_{0j}$ is the stress sharing ratio of the mini steel pipe pile and the jet grouting pile at the pile top; A_j is the cross-sectional area of the jet grouting pile, determined by (4); Z is the depth; L_s is the length of the mini steel pipe pile; L_j is the effective length of the jet grouting pile.

In addition, to coordinate the ultimate side friction at the interface between the mini steel pipe pile and the jet grouting pile with the ultimate side friction at the interface between the jet grouting pile and soil, it should also be noted that there is no shear failure between the mini steel pipe pile and the jet grouting pile under the condition of ensuring the material strength of the pile body [16–18]. Therefore, the bonding strength (ultimate side friction) at the interface between the mini steel pipe pile and the grouting pile should meet the following conditions:

$$Q_{0s} \le f_{su}, \tag{5}$$

$$f_{su} = U_s \int_0^{L_s} q_s(Z)dz \quad 0 \le Z \le L_s, \tag{6}$$

The composite foundation is used as a friction pile, so the pile top load shall not be greater than the ultimate side friction resistance of the jet grouting pile-soil interface.

$$Q_0 \le f_{ju}, \tag{7}$$

$$Q_0 = Q_{0s} + Q_{0j}, \tag{8}$$

$$f_{ju} = U_j \int_0^{L_j} q_j(Z)dz \quad 0 \le Z \le L_j, \tag{9}$$

In the equation, $q_s(Z)$ is the side friction resistance at the interface between the mini steel pipe pile and the jet grouting pile at depth Z; $q_j(Z)$ is the side friction resistance at the interface between the jet grouting pile and soil at depth Z; f_{su} is the ultimate side friction resistance at the interface between the mini steel pipe pile and the jet grouting pile; f_{ju} is the ultimate side friction resistance at the interface between the jet grouting pile and soil; U_s is the perimeter of the mini steel pipe pile; U_j is the perimeter of the jet grouting pile; Z is the depth; L_s is the length of the mini steel pipe pile; L_j is the effective length of the jet grouting pile; Q_0 is the pile top load.

According to the analysis results of the numerical model [19, 20], under the vertical compressive load, the maximum axial force of the jet grouting pile appears at the depth of 0 m

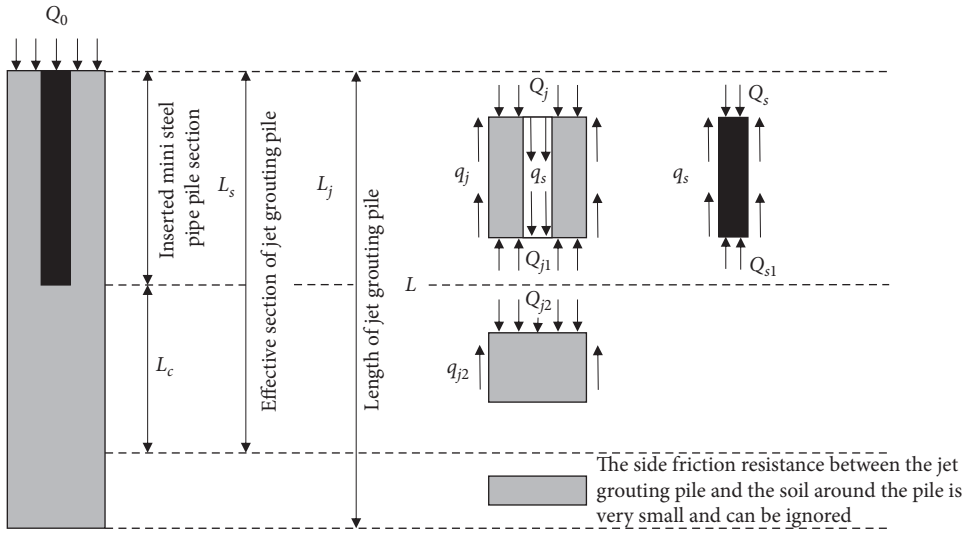

Figure 1: The schematic diagram of the force transfer mechanism of the composite foundation under vertical compressive load.

and the bottom of the mini steel pipe pile ($Z = L_s$). Therefore, when calculating the compressive bearing capacity of the composite foundation, the strength of the jet grouting pile needs to be checked according to equations (10) to (12).

$$Q_{0j} \le Q_{ju} = \sigma_{ju} A_j, \tag{10}$$

$$Q_j(L_s) \le R_2, \tag{11}$$

$$R_2 = \gamma_c Q_{ju}. \tag{12}$$

In the equation, σ_{ju} is the vertical compressive strength of the jet grouting pile (taking unconfined compressive strength); $Q_j(L_s)$ is the axial force of the jet grouting pile at depth L_s; R_2 is the maximum bearing capacity controlled by the pile body material of the "pure jet grouting pile section"; γ_c is the reduction coefficient of vertical compressive strength of the jet grouting pile. In case of lack of test data, $\gamma_c = 1$.

3. Assumption of the Interfacial Friction Distribution of the Composite Foundation under Vertical Compressive Load

According to relevant research results [20–22], the distribution law of side friction resistance between the mini steel pipe pile and the jet grouting pile and side friction resistance between the jet grouting pile and the soil around pile can be simply assumed, as shown in Figures 2 and 3, so as to facilitate design and calculation.

3.1. Assumption of Interfacial Friction Resistance Distribution between the Mini Steel Pipe Pile and the Jet Grouting Pile under Vertical Compressive Load. As can be seen from Figure 2, after simplifying the hypothesis, the side friction resistance between the mini steel pipe pile and the jet grouting pile presents a three-step distribution of small in the upper and large in the lower. The depth range of the first step is $0 \sim L_1$, and the average side friction resistance is τ_1; the depth range of the second step is $L_1 \sim L_2$, and the average side friction is τ_2; the depth range of the third step is $L_2 \sim L_s$, and the average side friction resistance is τ_3. The distribution of side friction resistance $q_s(Z)$ at the interface between the mini steel pipe pile and the jet grouting pile can be expressed by as

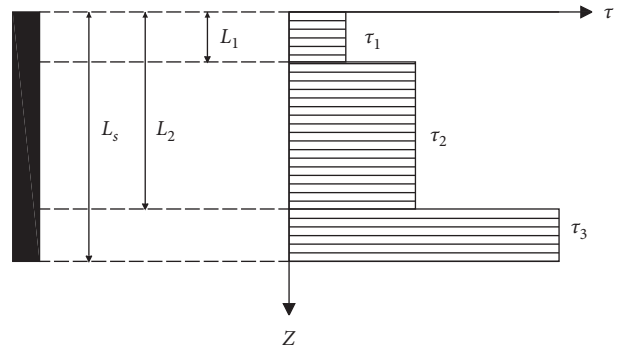

Figure 2: Distribution of interfacial friction resistance between the mini steel pipe pile and the jet grouting pile under overall compression mode.

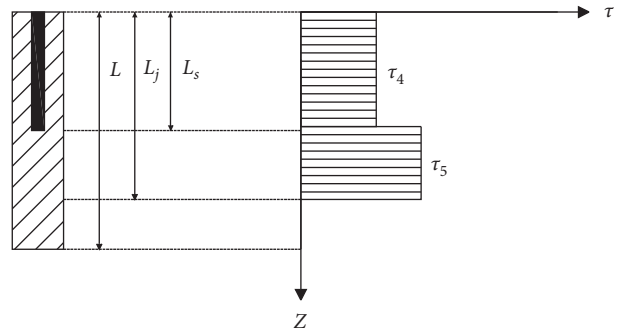

Figure 3: Distribution of interfacial friction resistance between the jet grouting pile and soil under overall compression mode.

$$q_s(Z) = \begin{cases} \tau_1 & (0 \le Z < L_1) \\ \tau_2 & (L_1 \le Z < L_2), \\ \tau_3 & (L_2 \le Z < L_s) \end{cases} \tag{13}$$

$$\tau_2 = 2\tau_1 = \xi\tau_3, \tag{14}$$

$$\tau_3 = \tau_u = \kappa\sigma_{ju}, \tag{15}$$

$$L_1 = \alpha D_s, \tag{16}$$

$$L_2 = L_s - L_1. \tag{17}$$

In the equation, $q_s(Z)$ is the side friction resistance between the mini steel pipe pile and the jet grouting pile; Z is the depth; τ_1, τ_2, and τ_3 are the average side friction resistance between the mini steel pipe pile and the jet grouting pile in different depth ranges. The value of ξ is based on the extent of the bonding force in the middle section of the mini steel pipe pile, and its proposed value is 0.05 according to the numerical simulation results. τ_u is the ultimate side friction resistance at the interface between the mini steel pipe pile and the jet grouting pile, which is related to the compressive strength of the jet grouting pile and the smoothness of the mini steel pipe pile κ, $\kappa = 0.15 \sim 0.4$; σ_{ju} is the compressive strength of the jet grouting pile; L_s is the length of the mini steel pipe pile; D_s is the outer diameter of the mini steel pipe pile; the value of α is taken according to the range of bonding force between the mini steel pipe pile and the jet grouting pile. When the whole composite foundation is compressed, $\alpha = 15$.

3.2. Assumption of the Distribution of Interficial Friction Resistance between the Jet Grouting Pile and Soil under Vertical Compressive Load. As can be seen from Figure 3, the side friction resistance at the interface between the jet grouting pile and the soil after the simplified assumption is divided into the upper and lower parts of "inserted mini steel pipe pile section" and "pure jet grouting pile section." The properties of the upper soil layer are often poor, and the ultimate side friction resistance at the upper part of the jet grouting pile-soil interface will be less than that at the lower part, which generally presents a two-step distribution. Therefore, the distribution of side friction resistance at the interface between the jet grouting pile and soil is

$$q_j(Z) = \begin{cases} \tau_4 & (0 \le Z < L_s) \\ \tau_5 & (L_s \le Z < L_j) \\ 0 & (L_j \le Z \le L). \end{cases} \tag{18}$$

In the equation, $q_j(Z)$ is the side friction resistance between the jet grouting pile and the soil around the pile; Z is the depth; τ_4 and τ_5 are the average ultimate side friction resistance of the jet grouting pile-soil interface in different depth ranges, which can be obtained according to the geological exploration report; L_s is the length of the mini steel pipe pile; L_j is the effective length of the jet grouting pile, and the value is shown in equation (1); L is the pile length of the jet grouting pile.

4. Axial Force Calculation of the Composite Foundation under Vertical Compressive Load

The above assumption of interfacial friction resistance distribution can be applied to the calculation of axial force of the composite foundation. According to the numerical simulation results, the mini steel pipe pile and the composite foundation can be regarded as the pure friction pile, and the bottom axial force can be regarded as 0. According to the force transmission mechanism of the composite foundation, the calculation equation of axial force of the composite foundation is established.

The cumulative sum of the side friction resistance of the mini steel pipe pile is equal to the upper load shared by its pile top. The axial force of the mini steel pipe pile can be expressed as

$$Q_s(Z) = Q_{0s} - U_s \int_0^Z q_s(Z)dZ. \tag{19}$$

Substituting equation (13) into equation (19), we obtain the following equation:

$$Q_s(Z) = \begin{cases} Q_{0s} - U_s\tau_1 Z & (0 \le Z < L_1), \\ Q_{0s} - U_s(\tau_1 L_1 + \tau_2 Z) & (L_1 \le Z < L_2), \\ \tau_3(L_s - Z) & (L_2 \le Z < L_s). \end{cases} \tag{20}$$

In the equation, $Q_s(Z)$ is the axial force of the mini steel pipe pile at different depths; τ_1, τ_2, and τ_3 are the average side friction resistance at the interface between the mini steel pipe pile and the jet grouting pile in different depth ranges; U_s is the perimeter of the mini steel pipe pile; Z is the depth; L_s is the length of the mini steel pipe pile; the values of L_1 and L_2 refer to equations (16) and (17), respectively.

The axial force of the jet grouting pile in the "inserted mini steel pipe pile section" is composed of the upper load shared by the top of the jet grouting pile, the side friction resistance of the mini steel pipe pile-jet grouting pile interface, and the side friction resistance of the jet grouting pile-soil interface, which can be expressed by equation (21).

The axial force distribution of the jet grouting pile is

$$Q_j(Z) = Q_{0j} + U_s \int_0^Z q_s(Z)dZ - U_j \int_0^Z q_j(Z)dZ. \tag{21}$$

Substituting equations (13) and (18) into equation (21), equation (22) can be obtained as follows:

$$Q_j(Z) = \begin{cases} Q_{0j} + \left(U_s\tau_1 - U_j\tau_4\right)Z & (0 \le Z < L_1), \\ Q_{0j} + \left(U_s\tau_1 - U_j\tau_4\right)L_1 + \left(U_s\tau_2 - U_j\tau_4\right)Z & (L_1 \le Z < L_2), \\ Q_{0j} + \left(U_s\tau_1 - U_j\tau_4\right)L_1 + \left(U_s\tau_2 - U_j\tau_4\right)L_2 + \left(U_s\tau_3 - U_j\tau_4\right)Z & (L_2 \le Z < L_3), \\ U_j\left(L_j - Z\right)\tau_5 & \left(L_s \le Z < L_j\right). \end{cases} \tag{22}$$

In the equation, $Q_j(Z)$ is the axial force of the jet grouting pile; Q_{0j} is the load shared on the top of the jet grouting pile; τ_1, τ_2, and τ_3 are the average side friction resistance at the interface between the mini steel pipe pile and the jet grouting pile in different depth ranges; U_s is the perimeter of the mini steel pipe pile; U_j is the perimeter of the jet grouting pile; τ_4 and τ_5 are the average side friction resistance of the jet grouting pile-soil interface in different depth ranges, which can be obtained according to the geological exploration report; L_s is the length of the mini steel pipe pile; L_j is the effective length of the jet grouting pile.

According to equations (20) and (22), under the overall compression mode of the composite foundation, the axial force distribution of the mini steel pipe pile and the jet grouting pile is shown in Figures 4 and 5, respectively.

5. Calculation of Bearing Capacity of the Composite Foundation under Vertical Compressive Load

The field vertical compression composite foundation in soil layers shown in Table 1 was selected for bearing capacity test and calculation comparative analysis. The calculation of the vertical compressive bearing capacity of the composite foundation is divided into the calculation of the ultimate bearing capacity controlled by the interface strength of the composite foundation and the calculation of the ultimate bearing capacity controlled by the material strength of the pile body of the composite foundation, and the smaller of the two is taken as the ultimate compressive load of the composite foundation. The parameters of the jet grouting pile and the mini steel pipe pile of the test pile are shown in Tables 2 and 3, respectively. The ultimate side friction resistance of each soil layer in the test site is shown in Table 1. The stratum distribution and composite profile at the test site is shown in Table 4.

According to the concept of the effective pile length, D_j is substituted into (1), and $\beta = 18$. It is calculated that the "effective section of pure jet grouting pile" $L_c = 10$m, and the calculation process is shown in equations (23) and (24), so there is no "invalid section of the jet grouting pile" in the composite foundation.

$$L_c = L_j - L_s = 10\text{m}, \tag{23}$$

$$\min\left\{\beta D_j, 10\right\} = \min\{18 \times 0.6, 10\} = 10\text{m} \ge L_c. \tag{24}$$

5.1. Maximum Bearing Capacity Controlled by Iinterface Strength. According to Table 1 and Figure 6, the ultimate side friction resistance of the jet grouting pile-soil interface calculated in combination with equation (9) is

$$f_{ju} = U_j \int_0^{L_j} q_j(Z)dz = 0.6\pi \times (1 \times 30 + 2 \times 23 + 6 \times 18 + 5 \times 40 + 6 \times 29) = 1051\text{kN}. \tag{25}$$

Combined with equation (6), equation (13), and Figure 2, the ultimate side friction resistance at the interface between the mini steel pipe pile and the jet grouting pile is calculated. Substituting the data in Table 3 into equations (16) and (17), respectively, $L_1 = 1.62$m and $L_2 = 8.38$m can be obtained, where $\alpha = 15$. According to Table 2, $\sigma_{ju} = 8\text{MPa} = 8000\text{kPa}$. $\kappa = 0.15 \sim 0.4$, so when taking $\kappa = (0.15 + 0.4)/2 = 0.275$ and substituting it into equation (15), $\tau_3 = 2200$kPa can be obtained; substituting $\xi = 0.05$ and τ_3 into equation (14), $\tau_2 = 110$kPa and $\tau_1 = 55$kPa can be obtained. Therefore, from equations (6) and (13), we obtain

$$\begin{aligned} f_{su} &= U_s \int_0^{L_s} q_s(Z)dz = U_s\left(L_1\tau_1 + \left(L_2 - L_1\right)\tau_2 + L_1\tau_3\right) \\ &= 0.108\pi \times (1.62 \times 55 + (8.38 - 1.62) \times 110 + 1.62 \times 2200) = 1492\text{kN}. \end{aligned} \tag{26}$$

Therefore, according to equations (25) and (26), $f_{ju} < f_{su}$, so the maximum bearing capacity controlled by the interface strength of the composite foundation under the overall compression mode is

$$R_i = f_{su} = 1051\text{kN}. \tag{27}$$

5.2. The Maximum Bearing Capacity of the Composite Pile Top Controlled by Pile Material Strength. The maximum bearing capacity of the mini steel pipe pile top under the control of pile material strength calculated by equation (2) and Table 3 is

$$\begin{aligned} Q_{0s} \le Q_{su} &= \sigma_{su}A_s = \sigma_{su}\left(T_sD_s - T_s^2\right)\pi \\ &= 358 \times 10^3 \times \left(0.008 \times 0.108 - 0.008^2\right)\pi = 900\text{kN}. \end{aligned} \tag{28}$$

The cross-sectional area of the jet grouting pile at the pile top calculated by equation (4) and Table 2 is

$$A_j = \left(D_j^2 - D_s^2\right)\frac{\pi}{4} = \left(0.6^2 - 0.108^2\right)\frac{\pi}{4} = 0.274\text{m}^2. \tag{29}$$

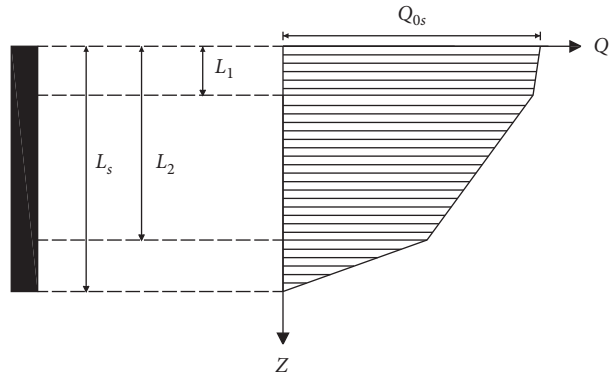

Figure 4: Axial force distribution of the mini steel pipe pile in the composite foundation under overall compression mode.

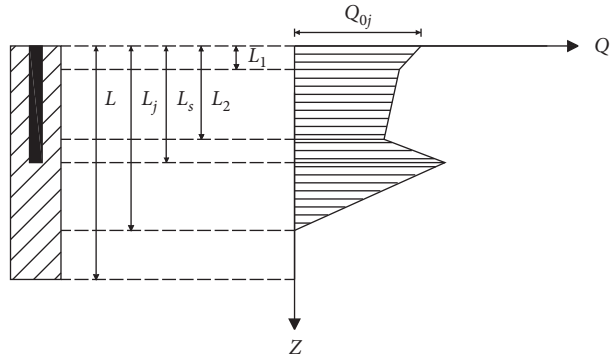

Figure 5: Axial force distribution of the jet grouting pile in the composite foundation under overall compression mode.

Table 1: Recommended value of ultimate side friction resistance of each soil layer.

Number	Name of soil	The state of the soil	Recommended value of ultimate side friction resistance/kPa
1	Silty clay	Plastic state, medium to high compressibility	30
2	Silty clay	Soft plastic state, medium to high compressibility	23
3	Mucky clay	High water content, high compressibility, flow plastic state	18
4	Silty clay with sand	Medium compressibility, slightly dense~moderately dense state	40
5	Silty clay	Soft plastic state, high compressibility	29

Table 2: Calculation parameters of the jet grouting pile.

Type of pile	Pile diameterD_j	Pile lengthL_j	Unconfined compressive strength	Tensile strength
Jet grouting pile	0.6 m	20 m	8 MPa	0.6 MPa

Table 3: Calculation parameters of the mini steel pipe pile.

Type of pile	Outer diameter D_s	Pile length L_s	Wall thickness T_s	Compressive yield strength	Tensile strength
Mini steel pipe pile	0.108 m	10 m	8 mm	358 MPa	410 MPa

Table 4: Comparison of measured and calculated bearing capacity of the composite foundation.

Load mode	Measured value of bearing capacity R_a/kN	Calculated value of bearing capacity R_c/kN	Absolute error/ kN	Relative error/%
Overall compressive strength of the composite foundation	1083	1051	32	3

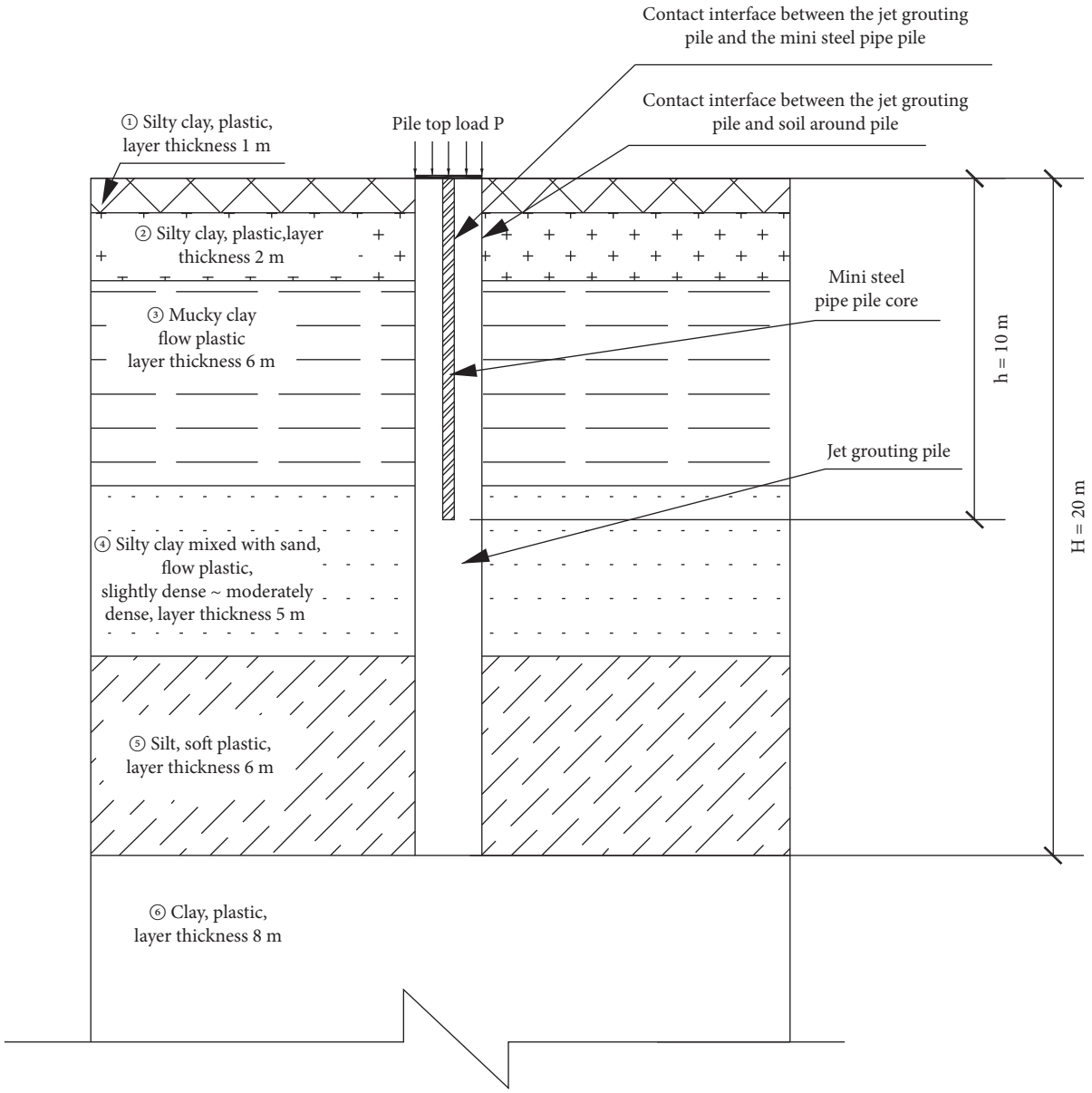

Figure 6: Stratum distribution and composite foundation profile at the test site.

The maximum bearing capacity of the jet grouting pile top under the control of pile material strength is calculated by substituting equation (10):

$$Q_{ju} = \sigma_{ju} A_j = 8 \times 10^3 \times 0.274 = 2192\text{kN}. \tag{30}$$

According to the numerical simulation analysis under the overall compression mode of the composite foundation, the pile top stress sharing ratio of the mini steel pipe pile and the jet grouting pile is $n_p = 140$ [7]. The load Q_{0j} shared by the top of the jet grouting pile calculated by equation (3) is

$$Q_{0j} = Q_{su} \frac{A_j}{A_s n_p} = 900 \times \frac{0.274}{0.002513 \times 140} = 700kN < Q_{ju} = 2192kN. \tag{31}$$

Therefore, the maximum bearing capacity of the pile top of the composite foundation under the overall compression mode is

$$R_t = Q_{su} + Q_{0j} = 900 + 700 = 1600\text{kN}. \tag{32}$$

5.3. Maximum Bearing Capacity of the "Pure Jet Grouting Pile Section". Using equation (22) and Table 1, the maximum bearing capacity of the "pure jet grouting pile section" under the control of ultimate side friction resistance of the jet grouting pile is

$$R_1 = Q_j(L_c) = U_j \int_{L_s}^{L_j} q_j(Z)dz = 0.6\pi \times (4 \times 40 + 6 \times 29) = 630\text{kN}. \tag{33}$$

Using equation (10), Q_{ju} of the "pure jet grouting pile section" can be obtained as follows:

$$Q_{ju} = \sigma_{ju} A_j = \sigma_{ju} D_j^2 \frac{\pi}{4} = 8 \times 10^3 \times 0.6^2 \times \frac{\pi}{4} = 2260\text{kN}. \quad (34)$$

We substitute equation (12), and $\gamma_c = 1.0$. The maximum bearing capacity of the jet grouting pile under the control of material strength is

$$R_2 = \gamma_c Q_{ju} = 1 \times 2260 = 2260\text{kN}. \quad (35)$$

Therefore, according to equations (33) and (35), $R_1 < R_2$, so the "pure jet grouting pile" section of the composite foundation will not be damaged under the overall compression mode.

Based on the above (1) to (3), $R_i = 1051\text{kN} < R_t = 1600\text{kN}$, so the ultimate bearing capacity of the composite foundation under the overall compression mode is

$$R_c = R_i = 1051\text{kN}. \quad (36)$$

5.4. Comparative Analysis of the Experimental Calculation of Vertical Compressive Bearing Capacity of the Composite Foundation. The comparison of measured and calculated bearing capacity of the composite foundation is shown in Table 4.

As can be seen from the table, under the overall compression mode, the measured test value of the bearing capacity of the composite foundation is 1083 kN. The calculated value determined by the calculation formula deduced under the assumed force distribution mode in this paper is 1051 kN, the absolute error between them is 32 kN, and the relative error is 3%. Therefore, both absolute error and relative error are very small. Therefore, the stress mode and calculation method of the jet grouting pile-mini steel pipe pile composite foundation proposed in this paper can meet the needs of engineering design and popularization and application of the composite foundation.

6. Conclusions

(1) Under the overall compression mode of the pile top of the composite foundation, the mini steel pipe pile and jet grouting pile jointly bear the upper load. According to the vertical force transmission characteristics of the composite foundation, the composite foundation can be divided into "inserted mini steel pipe pile section" and "pure jet grouting pile section" along the depth direction, and the jet grouting pile has "effective length." In the checking calculation of bearing capacity, the bearing performance of the mini steel pipe pile and jet grouting pile should be considered. Accordingly, the coordination effect of ultimate side friction resistance between the mini steel pipe pile and the jet grouting pile and ultimate side friction resistance between the jet grouting pile and soil should also be considered.

(2) The simplified hypothetical distribution diagram and calculation formula of interfacial friction resistance between the mini steel pipe pile and the jet grouting pile and interfacial friction resistance between the jet grouting pile and soil are put forward. The interfacial friction resistance between the mini steel pipe pile and the jet grouting pile presents a three-step distribution of small in the upper and large in the lower. The interfacial friction resistance between the jet grouting pile and soil generally presents a two-step distribution, and the ultimate side friction resistance at the upper part is less than that at the lower part.

(3) The mini steel pipe pile and the composite foundation can be regarded as pure friction piles, and the bottom axial force can be regarded as 0. According to the force transmission mechanism of the composite foundation, the calculation equation of the axial force of the composite foundation is established, the calculation formula of the axial force of the mini steel pipe pile and the jet grouting pile under the overall compression mode is deduced, and the axial force distribution diagram of the mini steel pipe pile and the jet grouting pile in the composite foundation is put forward.

(4) The calculation of the vertical compressive bearing capacity of the composite foundation is divided into the calculation of the ultimate bearing capacity controlled by the interface strength of the composite foundation and the calculation of the ultimate bearing capacity controlled by the material strength of the pile body of the composite foundation. The smaller of the two is taken as the ultimate compressive load of the composite foundation.

(5) The conclusions of this paper need to be further verified and improved by more engineering design examples.

Data Availability

The data supporting the conclusion of the article are shown in the relevant figures and tables in the article.

Conflicts of Interest

The authors declare that there are no conflicts of interest regarding the publication of this article.

Acknowledgments

This work was supported by Ningbo Tech. University.

References

[1] M. Aboutabikh, A. M. Soliman, and M. H. El Naggar, "Performance of hollow bar micropiles using green grout incorporating treated oil sand waste," *Journal of Building Engineering*, vol. 27, Article ID 100964, 2020.

[2] X. Liang, H. He, and Y. Zhang, "Optimization design of micro-piles in landslide safety protection based on machine learning," *Safety Science*, vol. 118, pp. 861–867, 2019.

[3] X. Li, Ming-Zhou Bai, M.-Z. Bai et al., "Application of carbon-fiber composite material in micropile structure," *Journal of Performance of Constructed Facilities*, vol. 34, no. 2, Article ID 04020017, 2020.

[4] J. Veludo, D. D. d. Costa, E. N. B. S. Júlio, and P. L. Pinto, "Bond strength of textured micropiles grouted to concrete footings," *Engineering Structures*, vol. 35, pp. 288–295, 2012.

[5] J. Veludo, E. N. B. S. Júlio, and D. Dias-da-Costa, "Compressive strength of micropile-to-grout connections," *Construction and Building Materials*, vol. 26, no. 1, pp. 172–179, 2012.

[6] F. Han, M. Prezzi, R. Salgado, and M. Zaheer, "Axial resistance of closed-ended steel-pipe piles driven in multilayered soil," *Journal of Geotechnical and Geoenvironmental Engineering*, vol. 143, no. 3, Article ID 04016102, 2017.

[7] N. Borthakur and A. K. Dey, "Evaluation of group capacity of micropile in soft clayey soil from experimental analysis using SVM-based prediction model," *International Journal of Geomechanics*, vol. 20, no. 3, Article ID 04020008, 2020.

[8] M. Khidri and L. Deng, "Field axial cyclic loading tests of screw micropiles in cohesionless soil," *Soil Dynamics and Earthquake Engineering*, vol. 143, p. 106601, 2021.

[9] M. T. Suleiman, L. Ni, J. D. Helm, and A. Raich, "Soil-Pile Interaction for a Small Diameter Pile Embedded in Granular Soil Subjected to Passive Loading," *Journal of Geotechnical and Geoenvironmental Engineering*, vol. 140, no. 5, Article ID 04014002, 2014.

[10] S. A. Davidow and D. G. Carr, "Micropile design and construction in a limited access wetland habitat," in *Proceedings of the Electrical Transmission and Substation Structures 2015*, pp. 35–45, Branson, Missouri, 2015.

[11] R. K. Gupta and S. Chawla, "Performance evaluation of micropiles as a ground improvement technique for existing railway tracks:finite-element and genetic programming approach," *International Journal of Geomechanics*, vol. 22, no. 3, Article ID 04021287, 2022.

[12] Z. Sun, L. Kong, and Y. Wang, "Seismic behaviour of a micropile-reinforced cut slope behind a cantilever retaining wall," *Soil Dynamics and Earthquake Engineering*, vol. 152, Article ID 107058, 2022.

[13] K. Boschi, Giulio di Prisco, C. G. di Prisco, and M. O. Ciantia, Micromechanical investigation of grouting in soils," *International Journal of Solids and Structures*, vol. 187, pp. 121–132, 2020.

[14] W. Zhang, Y. Li, A. T. C. Goh, and R. Zhang, "Numerical study of the performance of jet grout piles for braced excavations in soft clay," *Computers and Geotechnics*, vol. 124, Article ID 103631, 2020.

[15] A. M. Alnuaim, M. H. El Naggar, and H. El Naggar, "Performance of micropiled rafts in clay: numerical investigation," *Computers and Geotechnics*, vol. 99, pp. 42–54, 2018.

[16] H. Bayesteh, M. A. Fakharnia, and M. Khodaparast, "Performance of driven grouted micropiles: full-scale field study," *International Journal of Geomechanics*, vol. 21, no. 2, Article ID 04020250, 2021.

[17] L. Wen, G. Kong, Q. Li, and Z. Zhang, "Field tests on axial behavior of grouted steel pipe micropiles in marine soft clay," *International Journal of Geomechanics*, vol. 20, no. 6, Article ID 06020006, 2020.

[18] K. A. Kershaw and R. Luna, "Full-scale field testing of micropiles in stiff clay subjected to combined axial and lateral loads," *Journal of Geotechnical and Geoenvironmental Engineering*, vol. 140, no. 1, pp. 255–261, 2014.

[19] W. El Kamash, H. El Naggar, P. To, and N. Sivakugan, "The effect of long-term consolidation on foundations underpinned by micropiles in soft clay," *Ain Shams Engineering Journal*, vol. 13, no. 1, Article ID 101487, 2022.

[20] M. Esmaeili, M. Gharouni Nikand, and Farid Khayyer, "Experimental and numerical study of micropiles to reinforce high railway embankments," *International Journal of Geomechanics*, vol. 13, no. 6, pp. 729–744, 2013.

[21] M. S. Robison, "Excavation support and micropile underpinning in vail, Colorado," *GeoTrends*, pp. 112–118, 2010.

[22] K. Larsson and D. Jog, "Performance of micropiles used to underpin highway bridges," *Journal of Performance of Constructed Facilities*, vol. 28, no. 3, pp. 592–607, 2014.